PNAS

Supplementary Information for

Electrophysiological markers of memory consolidation in the human brain when memories are reactivated during sleep

Jessica D. Creery, David J. Brang, Jason D. Arndt, Adrianna Bassard, Vernon L. Towle, James X. Tao, Shasha Wu, Sandra Rose, Peter C. Warnke, Naoum P. Issa, and Ken A. Paller

This PDF file includes:

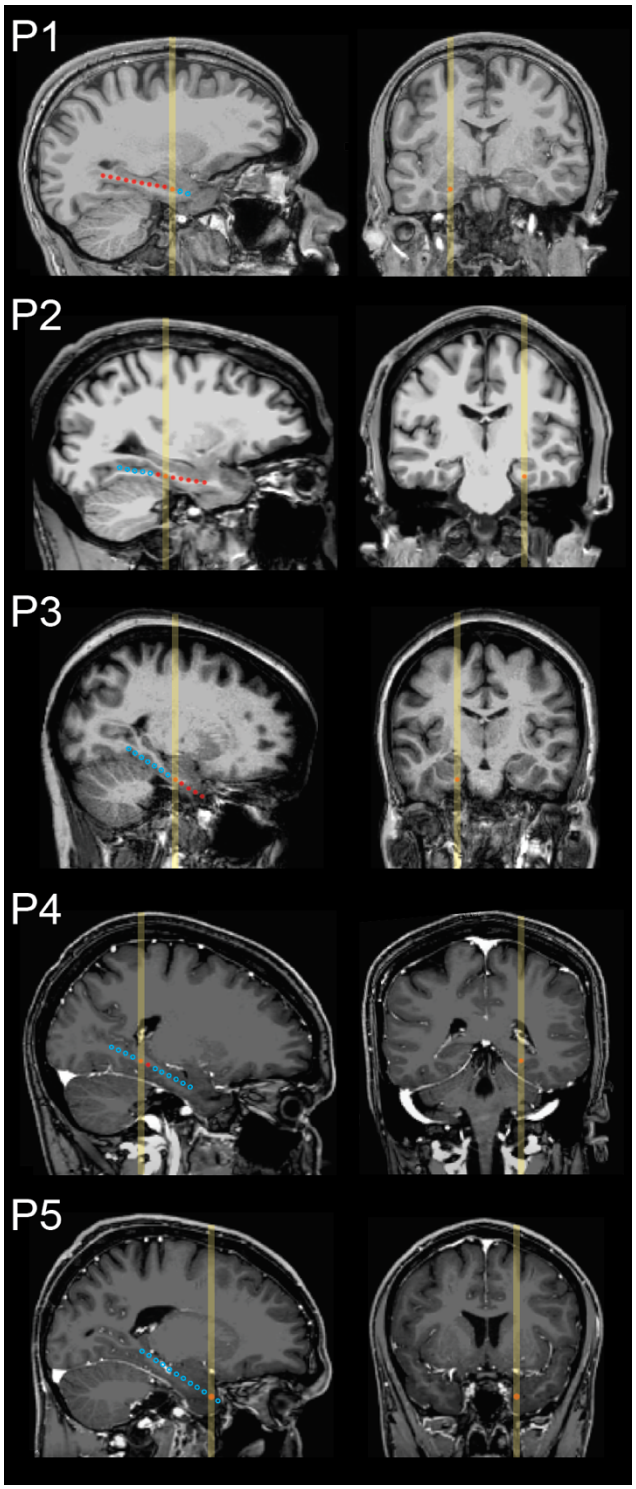

Fig. S1. Locations of intracranial electrodes used to monitor medial temporal activity in patients P1-P5. Depth probes were implanted through a small hole in the skull and targeted for the hippocampus, guided by anatomical information from pre-surgical MRI. Contacts were cylindrical, 1.25 mm in diameter and 2.5 mm long, situated 5 mm apart along each probe (measured center-to-center). Images on the left show a sagittal section that includes the estimated location of the contact selected for primary iEEG analysis as an orange circle. Locations of other contacts within the section are shown as red circles. Locations of contacts in adjacent sagittal sections were projected onto approximate locations in the section and shown as open blue circles. The yellow vertical line on each sagittal and coronal image indicates the location of the selected contact and corresponds to the approximate level of the section opposite.

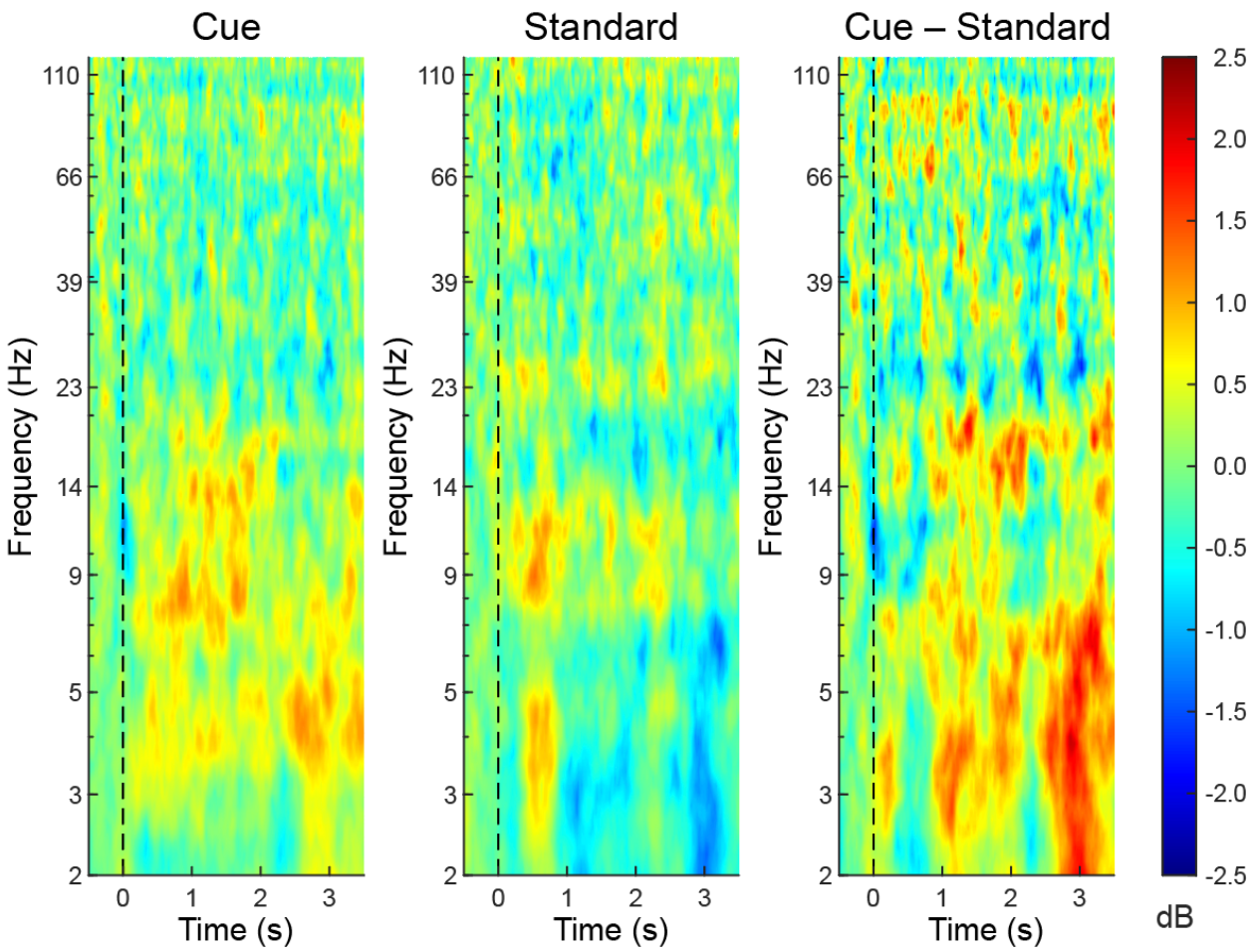

Fig. S2. Responses to sounds during sleep from the medial temporal location with the largest ERP amplitudes in each patient (locations and ERP values listed in Table S3). Time of sound onset indicated by dashed vertical lines (0 ms). Intracranial EEG responses to each sound presentation were analyzed to yield time-frequency responses across frequencies from 2-120 Hz (log scale), averaged for each condition within each patient, and then averaged across patients. Color indicates dB power, baseline-corrected using mean power over 500-ms interval prior to sound onset. Responses differed according to whether sounds were those used during the spatial learning task (cue sounds, left panel) or sounds not used during the spatial learning task (standard sounds, middle panel). Differences can be seen in the subtraction of responses to standard sounds from responses to cue sounds (right panel).

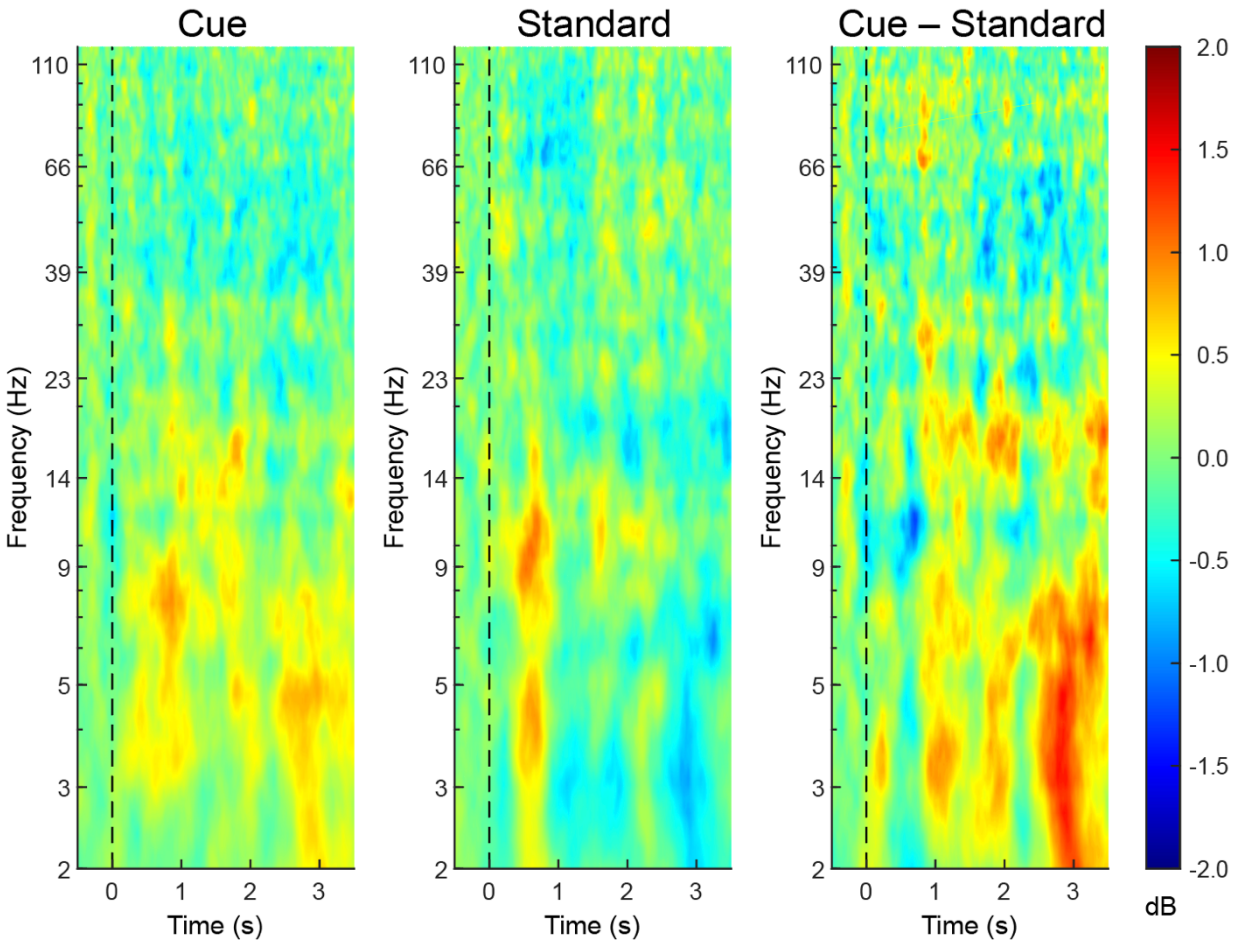

Fig. S3. Responses to sounds during sleep averaged over a set of five medial temporal locations (see Table S3), following the same format as in figure S2. Time of sound onset indicated by dashed vertical lines (0 ms). Intracranial EEG responses to each sound presentation were analyzed to yield time-frequency responses across frequencies from 2-120 Hz (log scale), averaged for each condition within each patient, and then averaged across patients. Color indicates dB power, baseline-corrected using mean power over 500-ms interval prior to sound onset. Responses differed according to whether sounds were those used during the spatial learning task (cue sounds, left panel) or sounds not used during the spatial learning task (standard sounds, middle panel). Differences can be seen in the subtraction of responses to standard sounds from responses to cue sounds (right panel).

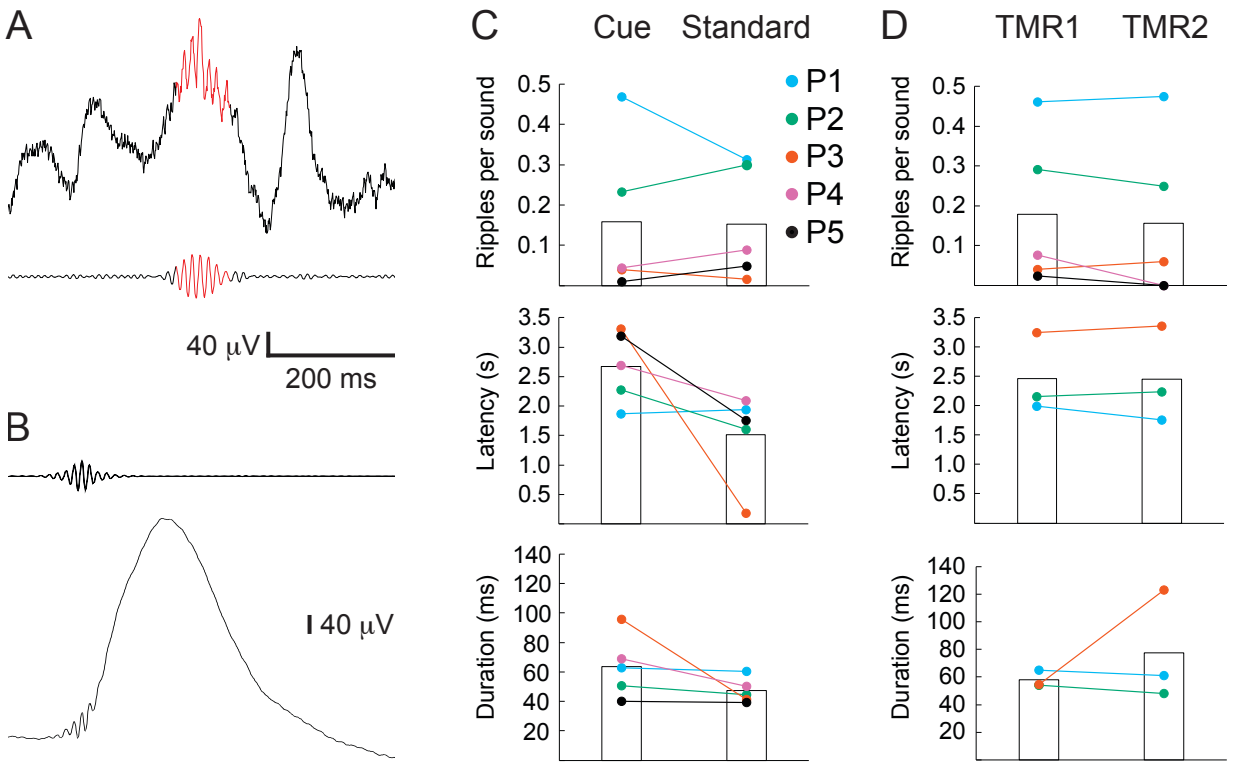

Fig. S4. Ripple results were analyzed from the one medial temporal contact in each patient with the highest ERP amplitude to all stimuli during sleep. Trials with artifacts from interictal spikes or high-frequency noise were removed prior to identifying ripples (full ripple-identification procedures are in Materials and Methods). (A) As a representative example, recordings from one patient (P1) show a single ripple, indicated in red. Data were filtered with a 60-Hz notch filter (upper trace) or with a bandpass at 80-100 Hz (lower trace). (B) A total of 396 ripples were identified in this patient and averaged time-locked to the largest positive peak, shown with and without filtering at 80-100 Hz (upper/lower, respectively), with a change in scaling for the latter. (C) Comparisons for ripples elicited by cue versus standard sounds during sleep showed no consistent effect on ripple rate, latency, or duration. (D) Comparisons between trials separated as a function of change in memory from before to after sleep also showed no consistent differences in ripple rate, latency, or duration. Because two patients showed no ripples for one condition, their data were not included in the latency and duration analyses.

Table S1. Individual patient demographics and electrophysiological monitoring details.

Patient	Age (years)	Gender	Epileptogenic Focus	Electrodes Implanted	Number of Contacts
P1	32	M	None identified	4 left temporal depth probes	48
P2	50	M	Left anterior medial temporal	2 bilateral temporal depth probes and 3 left temporal surface strips	42
P3	49	F	Left anterior medial temporal	1 left temporal depth probe and 3 left temporal surface strips	30
P4	21	F	Right anterior medial temporal	1 right temporal depth probe and 3 right temporal surface strips	28
P5	23	M	Right anterior medial temporal	1 right temporal depth probe and 6 right temporal and right parietal surface strips	42

Table S2. Sleep summary across patients based on scalp EEG data (values were based on best estimates for sleep staging, given that recordings were not typical polysomnographic recordings, sometimes with low-quality EEG and lacking electro-oculographic and electromyographic channels).

Stage	Mean (min)	SE (min)	Range (min)
N1	46.7	8.2	24.5 – 61.5
N2	158.2	23.0	85.5 – 227.5
N3	93.5	14.8	52.5 – 137.5
REM	28.2	5.3	10.5 – 40.0
Total	326.6	27.7	222.0 – 385.5

Table S3. Data from medial temporal probes for each patient (P1-P5). Contacts were on probes either in the left hemisphere (LH) or in the right hemisphere (RH). The five contacts used for the MLT cluster are shown in bold (with ** for the contact with the largest ERP amplitude and * for the other four contacts). Contacts RH2-5 in patient P4 and RH9-12 in patient P5 were omitted from analysis due to excessive seizure activity. Each contact was located within or close to the cortical region or brain structure listed. Measures are shown for differential EEG power for the post-stimulus interval (500-3500 ms) in dB, baseline-corrected, for theta power (4-8 Hz), sigma power (12-16 Hz), and gamma power (20-100 Hz). Lastly, ERP amplitudes (in microvolts) are shown for the maximal baseline-to-peak amplitude between 200-1200 ms after stimulus onset (collapsed for cue and standard stimuli delivered during sleep).

Patient	Contact	Location	Cue minus Standard			TMR1 minus TMR2			ERP
			Theta	Sigma	Gamma	Theta	Sigma	Gamma	
P1	**LH1***	Amygdala	0.26	-0.30	0.04	-0.93	1.55	0.26	12.0
	LH2*	Amygdala	0.23	0.03	0.05	-0.82	1.06	0.54	11.9
	LH3**	Hippocampus	1.41	0.44	0.24	-0.25	0.12	0.10	26.8
	LH4*	Hippocampus	1.25	0.21	0.15	-0.08	0.61	-0.12	16.4
	LH5*	Hippocampus	0.71	0.04	0.09	-0.88	0.32	0.46	13.9
	LH6	Hippocampus	0.03	-0.38	0.02	-0.38	0.47	0.71	13.0
	LH7	Hippocampus	0.01	-0.05	-0.26	-0.76	0.16	0.64	12.1
	LH8	Hippocampus	-0.05	0.23	-0.05	-0.96	0.08	0.86	12.3
	LH9	Parahippocampal	-0.02	0.65	0.28	-0.33	-0.28	0.77	10.1
	LH10	Lingual	0.19	1.04	0.17	0.87	0.50	0.42	6.1
	LH11	Lingual	0.38	1.01	0.03	1.15	0.56	0.28	0.4
	LH12	Lingual	0.11	1.03	-0.07	0.81	0.50	0.42	-1.5
P2	RH1	Entorhinal	-0.28	0.99	-0.15	1.56	-0.37	0.53	-21.3
	RH2	Amygdala	-0.37	1.29	-0.11	1.12	-0.28	0.59	-23.7
	RH3	Hippocampus	0.12	0.57	-0.21	1.78	0.95	1.02	-21.7
	RH4*	Hippocampus	-0.09	0.77	-0.69	0.16	1.52	0.21	-25.4
	RH5*	Hippocampus	0.28	0.14	-0.76	-0.92	1.97	0.04	-32.0
	RH6**	Parahippocampal	0.94	0.29	-0.40	-0.02	1.43	0.66	-36.0
	RH7*	Parahippocampal	0.71	-0.02	-0.31	0.82	1.67	0.82	-33.8
	RH8*	Parahippocampal	1.85	0.22	0.12	0.46	1.24	0.87	-16.8
	RH9	Parahippocampal	1.49	0.86	0.33	1.49	1.02	0.46	-16.1
	RH10	Lingual	1.69	0.74	0.27	1.37	1.25	0.46	-18.8
	RH11	Lingual	0.76	0.02	0.23	0.19	2.44	0.28	-18.5

	RH12	Lingual	0.40	0.05	0.09	-0.04	1.92	-0.10	-19.0
P3	LH1	Entorhinal	0.20	0.28	-0.24	-0.44	-0.40	-0.24	-19.8
	LH2	Entorhinal	-0.26	0.38	0.15	-0.24	0.03	0.22	-14.9
	LH3*	Entorhinal	0.01	0.41	-0.06	-0.41	-0.04	0.20	-17.6
	LH4*	Entorhinal	0.56	0.68	-0.06	-0.39	-0.17	0.19	-19.7
	LH5**	Entorhinal	0.00	0.58	0.04	-0.29	-0.38	0.07	-22.2
	LH6*	Parahippocampal	-0.27	-0.03	-0.07	-0.75	-0.31	0.19	-20.7
	LH7*	Parahippocampal	0.22	-0.27	-0.04	-1.13	-0.03	0.18	-20.0
	LH8	Parahippocampal	-0.06	-0.09	-0.04	-0.21	0.13	-0.05	-15.8
	LH9	Parahippocampal	-0.64	0.03	0.08	0.83	-0.32	-0.16	-17.1
	LH10	Fusiform	-0.16	-0.41	0.06	0.03	-0.89	-0.03	-15.4
	LH11	Lingual	0.00	0.01	0.06	0.32	-0.10	0.09	-15.7
	LH12	Lingual	-0.10	-0.07	0.07	0.42	0.36	-0.03	-20.6
P4	RH1	Hippocampus	-0.37	-0.48	-0.60	0.42	-0.30	-0.02	-48.7
	RH6*	Hippocampus	0.44	-0.42	-0.16	-0.27	-0.04	-0.23	-47.0
	RH7*	Hippocampus	0.66	-0.23	-0.11	-0.74	-0.12	0.03	-49.5
	RH8**	Hippocampus	0.74	0.22	-0.20	-0.24	-0.25	0.04	-50.5
	RH9*	Parahippocampal	0.67	0.73	-0.32	0.63	0.40	0.58	-46.7
	RH10*	Lingual	0.17	1.04	-0.23	0.48	0.39	0.55	-40.3
	RH11	Lingual	-0.14	0.48	-0.22	0.30	0.68	0.43	-36.7
	RH12	Lingual	-0.01	0.19	-0.36	0.30	1.41	0.13	-35.4
P5	**RH1***	Temporal pole	0.49	0.24	0.24	-0.78	0.74	0.35	-98.6
	RH2*	Entorhinal	0.63	0.34	0.33	-0.02	0.56	0.84	-103.0
	RH3**	Entorhinal	0.15	0.53	0.37	-0.01	0.60	0.51	-107.2
	RH4*	Entorhinal	0.13	0.10	0.15	-0.09	-0.06	0.36	-103.5
	RH5*	Amygdala	0.24	0.18	0.18	-0.28	-0.31	0.93	-93.0
	RH6	Hippocampus	0.38	0.48	0.51	-1.41	-0.42	0.79	-99.0
	RH7	Hippocampus	0.40	-0.48	0.55	-0.64	-0.78	0.65	-97.2
	RH8	Hippocampus	0.50	-0.31	0.30	-0.87	-2.18	0.61	-70.6

Table S4. The objects in the memory test. Human facial images shown below were altered to preserve anonymity. We used these images, each with a corresponding sound recording, in a task that required learning object-location associations. For each patient, we adjusted the number of objects in advance by estimating what would tax their abilities to a tolerable degree under the circumstances in the hospital (ranging from 10 to 20, Table 1). Objects were randomly selected from the set of 30 for each patient.